Trends in nanosecond melanosome microcavitation up to 1540 nm

Morgan S. Schmidt
Paul K. Kennedy
Gary D. Noojin
Rebecca L. Vincelette
Robert J. Thomas
Benjamin A. Rockwell

Trends in nanosecond melanosome microcavitation up to 1540 nm

Morgan S. Schmidt,[a,*] Paul K. Kennedy,[a] Gary D. Noojin,[b] Rebecca L. Vincelette,[b] Robert J. Thomas,[a] and Benjamin A. Rockwell[a]

[a]Human Effectiveness Directorate, Bioeffects Division, Optical Radiation Branch, 711th Human Performance Wing, Fort Sam Houston, Texas 78234, United States
[b]Engility Corporation, Fort Sam Houston, Texas 78234, United States

Abstract. Thresholds for microcavitation of bovine and porcine melanosomes were previously reported, using single nanosecond (ns) laser pulses in the visible (532 nm) and the near-infrared (NIR) from 1000 to 1319 nm. Here, we report average radiant exposure thresholds for bovine melanosome microcavitation at additional NIR wavelengths up to 1540 nm, which range from ∼0.159 J/cm^2 at 800 nm to 4.5 J/cm^2 at 1540 nm. Melanosome absorption coefficients were also estimated, and decreased with increasing wavelength. These values were compared to retinal pigment epithelium coefficients, and to water absorption, over the same wavelength range. Corneal total intraocular energy retinal damage threshold values were estimated and compared to the previous (2007) and recently changed (2014) maximum permissible exposure (MPE) safe levels. Results provide additional data that support the recent changes to the MPE levels, as well as the first microcavitation data at 1540 nm, a wavelength for which melanosome microcavitation may be an ns-pulse skin damage mechanism. © The Authors. Published by SPIE under a Creative Commons Attribution 3.0 Unported License. Distribution or reproduction of this work in whole or in part requires full attribution of the original publication, including its DOI. [DOI: 10.1117/1.JBO.20.9.095011]

*Address all correspondence to: Morgan S. Schmidt, E-mail: morgan.schmidt.ctr@us.af.mil

1 Introduction

Recently, the American National Standards Institute (ANSI) revised the standards for the maximum permissible exposure (MPE) for safe use of lasers under Z136.1.[1] The revisions included significant changes to the near-infrared (NIR) spectral region, and to the visible region in the nanosecond (ns) time regime. Our previous study reported NIR thresholds for ns-pulse melanosome microcavitation, which supported the changes made to the safety standards.[2] However, there is still a need for additional microcavitation data in the ns time regime, in order to support future updates to the ANSI safety standards. Therefore, due to the lack of ns-pulse threshold data at other NIR wavelengths of interest, we have expanded this study to determine additional average radiant exposure thresholds for microcavitation of isolated bovine melanosomes using ns laser pulses at wavelengths in the 800 to 1064 nm region, as well as at 1540 nm. Two different laser sources were used in order to probe NIR wavelengths of interest.

Melanosomes are found within both human skin and retinal pigment epithelium (RPE) layers of the eye. They are the main ocular light energy absorbers in the visible and NIR. As laser wavelengths increase into the mid-IR, water absorption increases and melanosome absorption decreases, depositing more absorbed energy in the cornea and anterior segments of the eye, and less in the posterior retinal tissue. The formation of small gaseous bubbles around melanosomes in the RPE, a process known as microcavitation, is the threshold-level damage mechanism for ns-pulse ocular exposures.[3–6]

The objective of this study was to more clearly illustrate the wavelength dependence of single-melanosome microcavitation thresholds for ns-pulse exposures covering the entire NIR regime. Results of this study were compared to the 2014[1] and 2007[7] ANSI Z136.1 MPE values, as well as to *in vivo* ns-pulse retinal damage threshold data in the visible and NIR. These results support the recent changes to the National Laser Safety Standards. Furthermore, we report the first microcavitation threshold data at 1540 nm, a wavelength for which melanosome microcavitation may be an ns-pulse skin damage mechanism.

2 Experimental Details and Procedures

Our procedure for bovine melanosome preparation followed the method of Dontsov et al.,[8] and these details can be found in our previous report.[2] In this study, additional wavelengths were investigated, including coherent emissions at 800, 900, 975, 1064, and 1540 nm. In order to observe the microcavitation events after exposure, a microscope containing two beam paths was used, a technique thoroughly described by Schmidt et al.[2] Although the OPO described in our previous publication is stable and can generate wavelengths out to 2400 nm, there was not enough energy per pulse to create the microcavitation events above 1200 nm. Therefore, multiple lasers were required at longer wavelengths to generate enough energy per pulse to create the cavitation event with increasing wavelength. Microcavitation events at 1540 nm were determined using emissions from a Megawatt (high-peak power) Er-glass laser (Hilton Head Island, South Carolina) with a custom Q-switch, designed by Taboda Research Instruments (San Antonio, Texas). This laser has a reasonably Gaussian spatial distribution, with 35-ns pulse duration and 3.5 J maximum energy per pulse.[9] The
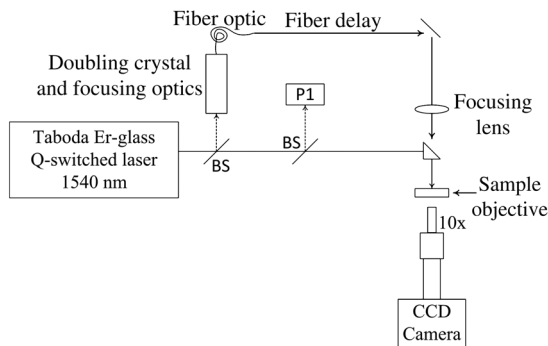
Fig. 1 Schematic of the laser and illumination setup for observing microcavitation bubble formation from irradiated melanosomes at 1540 nm. BS indicates beam splitters. P1 is a reference energy meter (dashed line represents 10% reflectance used at P1) and an additional detector is used at the sample source to determine energy delivered to the sample. The focused illumination beam was approximately 1 mm in diameter.

experimental setup for the 1540-nm data required changes from our previous report. Figure 1 is a schematic of the laser system and components.

The illumination beam was created by splitting (10%) and frequency doubling the 1540-nm laser beam, which resulted in 770-nm pulses. The 770-nm beam was launched into a 0.22 NA multimode 45-m fiber (FG105LCA Thorlabs), and focused at the sample surface, which optically triggered the CCD camera (Imperx Incorporated, Boca Raton, Florida). Time-resolved imagery of the microcavitation events was achieved by the 120-ns optical delay created by the fiber and free-space optical path differences. Previous research performed by Kelly[6] indicated that microcavitation bubbles expanded and collapsed in approximately 250 ns, and a 125-ns delay postexposure was a sufficient stroboscopic delay to observe cavitation events. Based on this previous research, similar delays were used postexposure for the current studies. Microcavitation images were collected using a Bobcat CCD camera (Imperx Incorporated, Boca Raton, Florida). Pre- and postcavitation images were also collected and used for background subtract from the exposure image for improved image quality. Beam diameter measurements were determined prior to each data collection set using the knife-edge technique. In each case, the spot size consisted of a $1/e^2$ Gaussian beam, which results in an average radiant exposure value. The NIR exposures (800 to 1064 nm) had an average beam diameter of $183 \pm 18~\mu m$. The average beam diameter at 532 nm was $295 \pm 22~\mu m$. The average beam diameter at 1540 nm was $305 \pm 31~\mu m$. It is important to note that although there were slight differences in pulse width (8 to 50 ns) at the different wavelengths used, we do not expect this to influence the measured cavitation thresholds. Microcavitation is the primary threshold-level retinal damage mechanism for pulsed exposures over the entire ns-time regime. Significant thermal diffusion only occurs on microsecond time scales and all ns-pulse exposures are within the thermal confinement region. Therefore, the slight variances in ns-pulse widths should not change the outcome of the study.

3 Results and Discussion

Probit analysis was the statistical method used to estimate the threshold (pulse) energy for laser-induced microcavitation (ED_{50}).[10,11] Binary (yes/no) data points were collected, the

ED_{50} energy, slope, and fiducial limits (FL) were determined at the 95% confidence level, and the ED_{50} radiant exposure was calculated by dividing the energy per pulse by the beam diameter. The radiant exposure (H) is computed by Eq. (1)

$$H = 4Q/\pi D_L^2, \tag{1}$$

where Q is the energy per pulse and D_L is the $1/e^2$ Gaussian beam diameter. An estimated total uncertainty of the average radiant exposure threshold was 16%. Data collection occurred on several successive days and was combined in order to produce a single ED_{50} threshold value at each wavelength. Table 1 summarizes the combined bovine microcavitation average radiant exposure thresholds, upper and lower FL, and Probit slope, from 532 to 1540 nm. The upper and lower FL limits represent the 95% confidence intervals. Values denoted by wavelength number[a] were determined in the previous study,[2] and values denoted by wavelength number[b] were determined in this study. Due to the significant water absorption in the mid-IR, the water layer above the melanosomes was taken into account to determine the microcavitation threshold of 4.5 J/cm² at 1540 nm. The actual radiant exposure was determined by calculating the transmission through our sample water layer of approximately 500 μm. At 1540 nm, water transmission is 55.3% based on Hale and Querry data,[12] with an absorption coefficient of 11.83 cm⁻¹. Thus, the observed cavitation threshold, corresponding to the radiant exposure at the surface of the water layer, was multiplied by the transmittance in order to find the actual radiant exposure at the melanosome. Figure 2 is a plot of bovine microcavitation thresholds as a function of wavelength,

Table 1 Probit threshold data for the combined trials for single, ns pulses at all wavelengths. The reported ED_{50} is an average radiant exposure for bovine melanosome microcavitation, determined from the ED_{50} pulse energy divided by the spot size area. The upper and lower fuducial limits (FL) represent the 95% confidence intervals. The 1540-nm value was corrected for the absorption of the water layer.

Wavelength (nm)	ED_{50} (mJ/cm²)	Lower FL (mJ/cm²)	Upper FL (mJ/cm²)	Probit slope	Number of shots
532[a]	99.2	96.1	102	10.9	453
800[b]	159	154	164	9.1	608
900[b]	203	197	209	8.63	698
975[b]	471	464	478	18.2	500
1000[a]	514	504	523	18.3	706
1064[b]	531	518	548	17.9	992
1100[a]	606	592	619	13.1	847
1200[a]	833	819	848	18.5	634
1319[a]	2650	2610	2690	13.4	1233
1540[b]	4504	4261	4792	15.2	165

[a]Values previously reported values from Schmidt et al.[2]
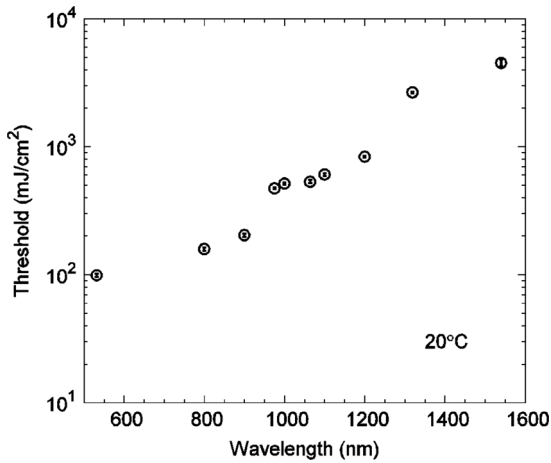[b]Values determined in this study.

Fig. 2 A comparison of radiant exposure thresholds of bovine melanosomes as a function of wavelength, on a log scale, from 532 to 1540 nm, at ambient temperature of 20°C. Error bars (smaller than the points as plotted) represent the upper and lower 95% fiducial confidence intervals.

on a log scale. Melanosome absorption coefficients were calculated from the threshold values in Table 1.

As previously reported, a first-order estimate of the melanosome absorption coefficient, μ_m, as a function of threshold radiant exposure, $F_{th}(T)$, measured at melanosome temperature T can be obtained using the following equation:[5,13]

$$T_{th} - T = [\mu_m F_{th}(T)]/[C_p/\rho], \qquad (2)$$

where C_p is the melanosome specific heat, ρ is the melanosome density, and T_{th} is the threshold temperature for bubble formation. Melanosome specific heat and particle density are $C_p = 2.55$ J/gm-°C and $\rho = 1.41$ gm/cm³.[13]

Cavitation data were collected at an ambient temperature of 20°C, and an estimated threshold temperature of $T_{th} = 150$°C was used based on the temperature-dependent, ns-pulse, melanosome microcavitation studies of Kelly[6] and Neumann and Brinkmann.[13] Using Eq. (2), one can solve for μ_m to determine absorption coefficients. Table 2 presents a comparison of the melanosome and RPE layer absorption coefficients, where the uncertainty in the melanosome data was estimated from both the experimental uncertainty of F_{th} and the threshold temperature (T_{th}) variability from the literature.[5,13,14] The RPE layer data are from Birngruber, et al.[15] As in Table 1, values denoted by wavelength number[a] were determined in the previous study,[2] and values denoted by wavelength number[b] were determined in this study. Figure 3 shows the wavelength dependence of the absorption coefficients for melanosomes, water, and the RPE layer, on a log scale. Note that in the visible and NIR, melanosome absorption coefficients are roughly an order of magnitude higher than corresponding RPE layer values. The results show melanosome and RPE layer absorption coefficients decreasing with increasing wavelength at roughly the same rate.

Figure 3 indicates that at 1540 nm, water and RPE layer absorption coefficients are similar (~ 10 cm⁻¹), even though the melanosome values are approximately an order of magnitude higher ($\sim 10^2$ cm⁻¹). The difference in these absorption coefficients are probably due to the high water content and low melanin concentration in the RPE layer, as a simple first-order calculation can demonstrate. RPE cells are approximately 20

Table 2 A comparison of the retinal pigment epithelium (RPE) and melanosome (μ_m) absorption coefficients as a function of wavelength. The RPE layer values were based on a fit to data extrapolated from Birngruber et al.[15] The uncertainty was estimated by combining the experimental uncertainty of F_{th} and the threshold temperature (T_{th}) variability from Refs. 5, 13, and 14.

Wavelength (nm)	RPE (cm⁻¹)	Melanosome (cm⁻¹)	Melanosome uncertainty (cm⁻¹)
532[a]	1381	4718	±896
800[b]	404	2943	±560
900[b]	255	2305	±438
975[b]	181	993	±188
1000[a]	161	925	±176
1064[b]	120	881	±167
1100[a]	102	763	±140
1200[a]	64	558	±106
1319[a]	41	176	±33
1540[b]	11.8	104	±29

[a]Values previously reported values from Schmidt et al.[2]
[b]Values determined in this study.

to 25 μm in diameter, and the RPE layer is roughly 15 μm thick. We can approximate the RPE cell as having a rectangular volume of 20 μm × 20 μm × 15 μm, or 6000 μm³. We can model the melanosome as a sphere 1 μm in diameter, giving a melanosome volume of 0.524 μm³. Finally, assuming 100 melanosomes per cell gives a melanin concentration of 0.87% (52.4/6000). The low melanin concentration minimizes
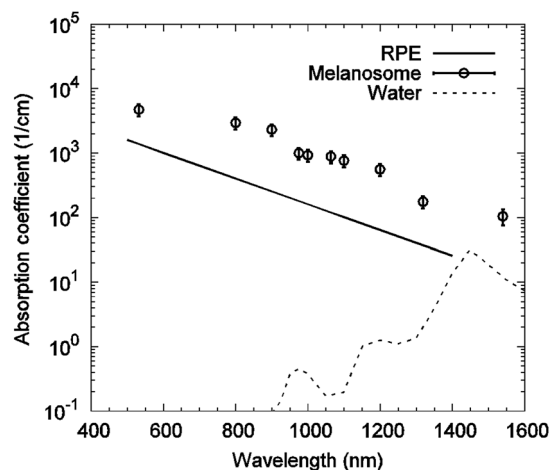

Fig. 3 Wavelength dependence of water, melanosome, and retinal pigment epithelium (RPE) layer absorption coefficients on a log scale. Although the melanosome absorption coefficients are roughly an order of magnitude higher than the RPE layer values, both coefficients decrease with increasing wavelength at approximately the same rate.

the effect of the higher melanosome absorption coefficient on the total RPE layer absorption, keeping the latter close to the water value at this wavelength. As shown in Fig. 2, decreasing melanosome absorption in the mid-IR does cause a significant increase in the microcavitation threshold radiant exposure from 1319 to 1540 nm.

This paper reports the first melanosome microcavitation threshold values at 1540 nm. These data show that despite reduced melanin absorption in the mid-IR, it is possible to create melanosome microcavitation events at 1540 nm, assuming a sufficiently high-radiant exposure can reach the melanosome. For high-peak power, ns-pulse, 1540-nm skin exposures, resident dermal melanosomes could receive doses producing microcavitation that may damage skin. A previous 1540-nm, ns-pulse, threshold skin study by Lukashev et al.[16] reported an ED_{50} value for minimal visible lesions (MVLs) of 3.0 J/cm^2. We should note that there are structural and chemical differences between retinal melanosomes and skin melanosomes, which will probably produce different microcavitation thresholds.

This, in turn, might explain the difference between the measured, ns-pulse, $MVL-ED_{50}$ for skin and the ns-pulse (retinal melanosome) microcavitation threshold reported in this study.

Whatever the threshold-level skin damage mechanism might be, microcavitation damage clearly will not occur for RPE melanosomes, since water absorption in the anterior portions of the eye would reduce 1540-nm ocular transmission to the retina to virtually zero. Only the cornea and lens would be damaged at this wavelength and these energies, so RPE microcavitation is not currently considered a likely ocular damage mechanism for ns-pulse mid-IR laser exposures. Very few corneal damage studies have been performed in the 1540-nm wavelength range for ns exposures. In one example, Lund et al.[17] reported an $MVL-ED_{50}$ corneal damage threshold of 21 J/cm^2 $(1/e)$ at 1540 nm with a 50-ns single pulse.

As a final validation of our results, a comparison between melanosome microcavitation threshold radiant exposure values and total intraocular energy (TIE) values, corresponding to measured retinal damage thresholds *in vivo*, was performed for the

Table 3 Comparison of rhesus monkey *in vivo* ED_{50} total intraocular energy (TIE) values from 532 to 1319 nm in the nanosecond pulse regime and a range of corneal irradiance diameters.[19–27] These data are plotted in Fig. 4, and compared with estimated microcavitation TIE thresholds in the same wavelength regime based on a 3-mm diameter $(1/e^2)$ Gaussian beam entering a rhesus eye.

| Wavelength (nm)	Pulse duration (ns)	Corneal irradiance diameter (mm)	Damage site	Observation time	ED_{50} TIE (μJ)	Range (μJ)	Reference
532	4	2.5	Retina	24 h	0.90	0.6 to 1.35	19
532	3.5	3	Retina	24 h	0.51	0.38 to 0.65	20
532	3.5	6	Retina	24 h	0.57	0.29 to 0.79	21
694.3	30	3	Retina	1 h	16.90	14.5 to 19.6	22
694.3	50	4 to 5	Retina	1 h	11.20	9 to 15.1	23
799.5	16	4 to 5	Retina	1 h	16.7	14.8 to 18.8	23
810.2	12	4 to 5	Retina	1 h	28.4	25.4 to 31.8	23
850.2	11		Retina	1 h	9.10	7.8 to 10.7	24
850.2	180	4 to 5	Retina	1 h	12	9.5 to 15.1	23
850.3	11	4 to 5	Retina	1 h	8.5	7.26 to 9.96	23
867	7		Retina	2 h	5.2	4.4 to 6.0	23
880	14		Retina	1 h	6.30	5.2 to 7.7	24
899.7	6		Retina	1 h	4.3	3.4 to 5.3	23
899.9	10	4 to 5	Retina	1 h	6.62	5.69 to 7.7	23
904	8	4 to 5	Retina	1 h	15.2	14.2 to 18.7	23
912	7	4 to 5	Retina	1 h	6.54	5.57 to 7.68	23
912	7		Retina	1 h	5.50	4.6 to 6.7	24
1064	7	3	Retina	1 h	28.70	22.3 to 39.3	25
1064	7	3	Retina	24 h	19.10	17.3 to 21.2	26
1319	50	4.5	Retina	24 h	19300	17300 to 21200	27
1319	50	4.5	Retina	24 h	22000	20100 to 24600	28
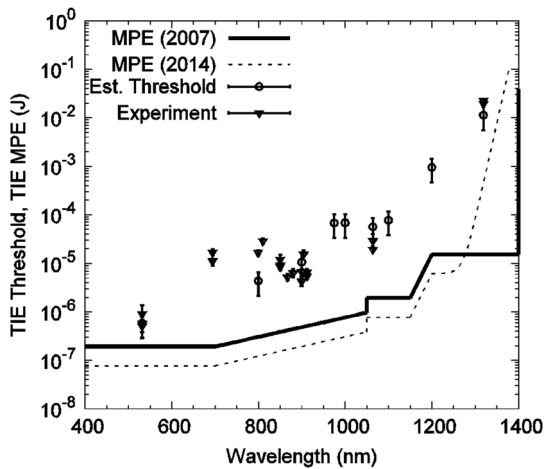
Fig. 4 Comparison of estimated and experimental total intraocular energy (TIE) thresholds with ANSI Z136.1-2007 and ANSI Z136.1-2014 maximum permissible exposure (MPE) limits for 1 to 100 ns pulses, expressed in terms of permissible TIE. The TIE MPE is defined as the MPE given in terms of the corneal radiant exposure multiplied by the area defined by a 7 mm pupillary aperture.[1,7] Estimated (microcavitation) TIE thresholds are based on a 3-mm diameter $(1/e^2)$ Gaussian beam entering a rhesus eye. Experimental TIE data, for *in vivo* rhesus studies, are from referenced sources in Table 3.[19–27]

extended microcavitation dataset, with the exception of 1540 nm. Prior to comparing the two datasets, however, the microcavitation radiant exposure thresholds had to be converted into their corresponding TIE values. The microcavitation TIE represents the energy delivered to the corneal plane, which should result in retinal damage due to RPE microcavitation. For this calculation, the threshold radiant exposure at the RPE layer was assumed to be equivalent to our single-melanosome thresholds, listed in Table 1. Next, the retinal radiant exposure threshold was combined with the estimated retinal spot size and ocular transmission values for the rhesus monkey, based on the model of Vincelette et al.,[18] to back calculate the threshold energy at the cornea. The Vincelette model estimates retinal beam diameter based on focusing of a 3-mm diameter Gaussian beam entering an emmetropic rhesus eye. A rhesus eye model was chosen for this calculation so that our microcavitation TIE values could be validated by direct comparison to retinal MVL-ED$_{50}$ TIE values measured for visible and near-IR ns-pulse exposures in the rhesus eye.

Table 3 lists the *in vivo* rhesus MVL-ED$_{50}$ TIE values used for comparison to our microcavitation data. These represent a variety of ns-pulse experimental studies, for differing corneal beam diameters, over the wavelength range from 532 to 1319 nm.[19–27] Figure 4 compares the estimated microcavitation TIE thresholds, calculated for a 3-mm diameter Gaussian beam entering a rhesus eye, to the experimental *in vivo* TIE values of Table 3. These two datasets are also compared to the 2014[1] and 2007[7] ANSI Z136.1 MPE limits for 1 to 100 ns pulses, expressed in terms of permissible TIE. The TIE MPE is defined as the MPE given in terms of the corneal radiant exposure multiplied by the area defined by a 7-mm pupillary aperture.[1,7] It is evident that the estimated TIE values from microcavitation radiant exposure thresholds mimic the trends in the MVL studies of various authors. Error bars for estimated TIE values represent ~51% uncertainty, based on a ±0.25 diopter deviation from emmetropia, uncertainty in retinal transmission, and uncertainty

in energy measurements.[28] The uncertainty for the *in vivo* measurements corresponds to the upper and lower FL found in Table 3.

4 Conclusions

This work supplements and extends our previous study,[2] which presented the first threshold data ever reported in the literature for ns-pulse melanosome microcavitation in the near-IR. Here, we report additional ns-pulse microcavitation thresholds, measured in the critical 800 to 1064 nm region, with the goal of more clearly illustrating the wavelength dependence of ns-pulse melanosome microcavitation over the entire near-IR regime. We also report the first microcavitation threshold data at 1540 nm, a wavelength for which melanosome microcavitation may be a ns-pulse skin damage mechanism. As before, the threshold radiant exposure data was used to estimate melanosome absorption coefficients and these were compared to absorption coefficients for water and the RPE layer, over the entire wavelength range from 532 to 1540 nm. The 1540-nm cavitation thresholds were significantly higher than 1319-nm values, indicating lower melanosome absorption coefficients and higher skin damage thresholds in the mid-IR. Finally, the microcavitation data was compared to ns-pulse ANSI MPE values and to *in vivo* ns-pulse retinal damage thresholds in the visible and NIR. Trends in the microcavitation data are consistent with those in MVL studies from the literature, and these results provide additional data to support the recently updated ANSI Z136.1.

References

1. ANSI, *American National Standard for Safe Use of Lasers*, Laser Institute of America, Orlando, Florida (2014), ANSI Z136.1-2014.
2. M. S. Schmidt et al., "Trends in melanosome microcavitation thresholds for nanosecond pulse exposures in the near infrared," *J. Biomed. Opt.* **19**(3), 035003 (2014).
3. B. J. Lund, D. J. Lund, and P. R. Edsall, "Damage threshold from large retinal spot size repetitive-pulse laser exposures," *Health Phys.* **107**(4), 292–299 (2014).
4. B. S. Gerstman et al., "Laser-induced bubble formation in the retina," *Laser Surg. Med.* **18**, 10–21 (1996).
5. R. Brinkmann et al., "Origin of retinal pigment epithelium cell damage by pulsed laser irradiance in the nanosecond to microsecond time regimen," *Lasers Surg. Med.* **27**(5), 451–464 (2000).
6. M. W. Kelly, "Intracellular cavitation as a mechanism of short-pulse laser injury to the retinal pigment epithelium," PhD Dissertation, Tufts University (1997).
7. ANSI, *American National Standard for Safe Use of Lasers*, Laser Institute of America, Orlando, Florida (2007), ANSI Z136.1-2007.
8. A. E. Dontsov, R. D. Glickman, and M. A. Ostrovsky, "Retinal pigment epithelium pigment granules stimulate the photo-oxidation of unsaturated fatty acids," *Free Radicals Biol. Med.* **26**(11–12), 1436–1446 (1999).
9. J. Taboada et al., "100-megawatt Q-switched Er-glass laser," *Proc. SPIE* **6100**, 61000B (2006).
10. D. J. Finney, *Probit Analysis*, Cambridge University Press, New York (1971).
11. C. P. Cain, L. Manning, and G. D. Noojin, "A comparison of various probit methods for analyzing yes/no data on a log scale," AF Technical Report AL/OE-TR-1996-0120, USAF Armstrong Laboratory, p. 46 (1996).

12. G. M. Hale and M. R. Querry, "Optical constants of water in the 200-nm to 200-μm wavelength region," *Appl. Opt.* **12**(3), 555–563 (1973).
13. J. Neumann and R. Brinkmann, "Boiling nucleation on melanosomes and microbeads transiently heated by nanosecond and microsecond laser pulses," *J. Biomed. Opt.* **10**(2), 024001 (2005).
14. J. Neumann and R. Brinkmann, "Nucleation dynamics around single microabsorbers in water heated by nanosecond laser irradiation," *J. Appl. Phys.* **101**(11), 114701 (2007).
15. R. Birngruber, F. Hillenkamp, and V. P. Gabel, "Theoretical investigations of laser thermal retinal injury," *Health Phys.* **48**, 781–796 (1985).
16. A. V. Lukashev et al., "Morphological and histological changes on skin induced by 1540 nm laser irradiation," *Proc. SPIE* **2974**, 36–45 (1997).
17. D. J. Lund et al., "Ocular hazards of the Q-switched erbium laser," *Invest. Opthalmol.* **9**, 463–470 (1970).
18. R. L. Vincelette et al., "Thermal lensing in ocular media exposed to continuous-wave near-infrared radiation: the 1150–1350-nm region," *J. Biomed. Opt.* **13**(5), 054005 (2008).
19. C. P. Cain et al., "Visible retinal lesions from ultrashort laser pulses in the primate eye," *Invest. Ophthalmol. Visual Sci.* **36**(5), 879–888 (1995).
20. B. J. Lund, D. J. Lund, and P. R. Edsall, "Laser-induced retinal damage threshold measurements with wavefront correction," *J. Biomed. Opt.* **13**(6), 064011 (2008).
21. B. J. Lund, D. J. Lund, and P. R. Edsall, *Damage Threshold from Large Retinal Spot Size Repetitive-Pulse Laser Exposures*, Laser Institute of America (2009).
22. G. D. Frisch, E. S. Beatrice, and R. C. Holsen, "Comparative study of argon and ruby retinal damage thresholds," *Invest. Ophthalmol Visual Sci.* **10**(11), 911–919 (1971).
23. D. J. Lund and E. S. Beatrice, "Near infrared laser ocular bioeffects," *Health Phys.* **56**(5), 631–636 (1989).
24. D. J. Lund, E. S. Beatrice, and S. T. Schuschereba, "Bioeffects data concerning the safe use of GaAs laser training devices," in *Combat Ocular Problems*, E. S. Beatrice, Ed., pp. 15–29, Letterman Army Institute of Research, San Francisco, California (1982).
25. C. P. Cain et al., "Thresholds for visible lesions in the primate eye produced by ultrashort near-infrared laser pulses," *Invest. Ophthalmol. Visual Sci.* **40**(10), 2343–2349 (1999).
26. C. P. Cain et al., "Visible lesion thresholds from near-infrared pico and nanosecond laser pulses in the primate eye," *Proc. SPIE* **2975**, 133–137 (1997).
27. J. A. Zulich et al., "Ocular effects and safety standard implications for high-power lasers in the $1.3 - 1.4$ μm wavelength range," USAF Technical Report No. AFRL-HE-BR-TR-2004-0187, pp. 1–16, AFRL/HEDO, San Antonio (2004).
28. D. H. Sliney et al., "What is the meaning of threshold in laser injury experiments? Implications for human exposure limits," *Health Phys.* **82**(3), 335–347 (2002).

Biographies for the authors are not available.